

Spatial superpositions of Gaussian beams

Darryl Naidoo^{a,b†}, Thomas Godin^c, Michael Fromager^d, Kamel Aït-Ameur^d and Andrew Forbes^{a,b}

^aCSIR National Laser Centre, P. O. Box 395, Pretoria 0001, South Africa

^bLaser Research Institute, University of Stellenbosch, Stellenbosch 7602, South Africa

^cInstitute FEMTO-ST, 16 Route de Gray, Besançon 25030, France

^dCIMAP—ENSICAEN, 6, bd Maréchal Juin, 14050 Caen Cedex 4, France

ABSTRACT

We explore an interferometric beam shaping technique that considers the coaxial superposition of two Gaussian beams. This technique is traditionally implemented in a Mach-Zehnder interferometer; however, to avoid phase shift drift due to vibrations and thermal effects we employ amplitude and phase modulation with a spatial light modulator (SLM) to achieve the beam shaping. We consider two Gaussian beams of equal but opposite curvature that possess the same phase and width incident on a focusing lens. At the plane of the lens we obtain a multi-ringed beam with a central intensity maximum which develops into a multi-ringed beam with a central null at the focal plane of the lens. The interesting feature of this beam is that it possesses two focal spots on either side of the focal plane of the lens. We investigate obstructing the beam at the focal plane of the lens and by carefully selecting the free parameters we obtain an unobstructed second focus while the equivalent Gaussian beam is sufficiently obstructed.

Keywords: cosine-Gaussian beam, Optical bottle beam, bi-axial focusing.

1. INTRODUCTION

In general the output mode of many commercial laser systems deliver a beam with a Gaussian intensity profile, however, this mode is not always ideally suited to the application at hand. This deficiency is overcome by typically shaping the laser beam external to the cavity through the use of transparent diffractive optical elements (DOE). Laser beam shaping through DOE's has been extensively researched whether the DOE is programmable or not^{1,2}. Programmable DOE's are based on liquid crystal optical valves or deformable mirrors which have the advantage of being very flexible in that they are controlled in an all digital approach. Non-programmable DOE's, however, consist of a transparent material in which an adequate relief is etched giving rise to a desired phase shift profile where the relief may be discrete or continuous. Our objective is to study a supplementary technique of laser beam shaping; interferometric laser beam shaping which contrasts with the usual one based on diffraction. Interesting features from laser beam shaping using interferometric techniques have been already demonstrated in literature in the generation of a focal spot having a size smaller than that of a Gaussian beam from the axial superposition of two Gaussian beams³ and the generation of optical vortices⁴⁻⁶.

The principal contributions in the area of laser beam shaping based on interferometric techniques are dedicated to the generation of optical bottle beams (OBB). This beam is characterised by a central hollow region that is surrounded by higher intensity light rings in the three principal directions. The OBB has been shown to be very useful for trapping of particles having a refractive index lower than the surrounding medium⁷. Techniques in the generation of OBB's include 1: transforming a LG_{00} beam into a LG_{20} by the use of computer generated holograms, where it has been found that the optical barrier along the axis of the beam is roughly three times larger in the radial direction⁸. 2: Directly inside a laser comprised of a degenerate set of transverse modes LG_{p0} (with $p=0, 3, 6\dots$). These modes interfere near the focal plane of a converging lens as they have the same frequency^{9,10}. 3: From the interference of two Bessel beams which are generated by using a SLM¹¹ and 4: by the destructive interference of two Gaussian beams with different waists that are focused in the same plane¹².

[†] Corresponding author: Darryl Naidoo; tel: +27 12 841 3797; fax: +27 12 841 3152; email: dnaidoo3@csir.co.za

In this paper, we explore the coaxial superposition of two coherent Gaussian beams where the two beams have the same width but opposite curvature and focus in different planes after passing through a focusing lens¹³. At the plane of the lens we obtain a multi-ringed beam with a central intensity maximum which develops into a multi-ringed beam with a central null (OBB) at the focal plane of the lens. We will also explore the bi-axial focusing property of this beam with an on-axis obstruction at the focal plane of the lens. Traditionally, this technique is implemented in a Mach-Zehnder interferometer; however, to avoid phase shift drift due to vibrations and thermal effects we employ amplitude and phase modulation with an SLM to achieve the beam shaping.

2. SUPERPOSITION OF GAUSSIAN BEAMS

The coaxial superposition of two Gaussian beams of equivalent width but opposite curvature is generated by modulating some Gaussian beam with a suitable transmission function and the electric field of such a beam may be expressed as:

$$u_{CGB} = E_0 \cos(\beta r^2) \exp\left(-\frac{r^2}{w^2}\right), \quad (1)$$

where w is the Gaussian beam width and β is a quantity that is inversely proportional to some squared length where we arbitrarily set $\beta=2\pi N/w^2$ with $N \in \Re$. The multi-ringed beam also described as a cosine-Gaussian beam (CGB) in Eq. (1) contains a modulating term $\cos(\beta r^2)$ having its origin in the interference between two spherical wavefronts with opposite radii of curvature and not in a planar phase difference between the two Gaussian beams. The modulated Gaussian field in Eq. (1) may be equally expressed as the coaxial superposition of two Gaussian beams having the same width w and opposite radii of curvature as:

$$u = \frac{E_0}{2} \exp\left(-\frac{r^2}{w^2}\right) \left(\exp\left(-\frac{i k r^2}{2R}\right) + \exp\left(\frac{i k r^2}{2R}\right) \right), \quad (2)$$

where $k=2\pi/\lambda$ and R is the radius of curvature. If we expand the transmission function in Eq. (1), $\cos(\beta r^2) = 1/2 (\exp(i\beta r^2) + \exp(-i\beta r^2))$, and equate the expanded expression to that in Eq. (2), we find a relationship for the radius of curvature to the parameter N , expressed as:

$$R = \frac{w^2}{2\lambda N}. \quad (3)$$

The selection of the parameter N is particularly significant in determining the spatial properties of the CGB upon passing through a focusing lens. There are two cases that occur simultaneously to the field u_{CGB} (Eq. (1)) when passed through a lens of focal length f . Starting at the plane of the lens, the first case is that one of the Gaussian beams will *always* focus at some position along the propagation axis, the second case considers the second Gaussian beam and is comprised of three scenarios: 1. The beam will also focus at some position along the propagation axis, 2. The beam will be collimated during propagation and 3. The beam will diverge during propagation. It must be noted that for scenario 1, the second focus will always be larger than the first and these scenarios are illustrated in Fig. 1. Scenario 2 is achieved by equating the curvature of the field to the focal length of the lens, $R=f$ and from Eq. (3), we find that this condition equates to:

$$N = \frac{w^2}{2\lambda f}. \quad (4)$$

Scenario 1 is achieved for values of N less than that in Eq. (4) and scenario 3 is achieved for values of N larger than that in Eq. (4).

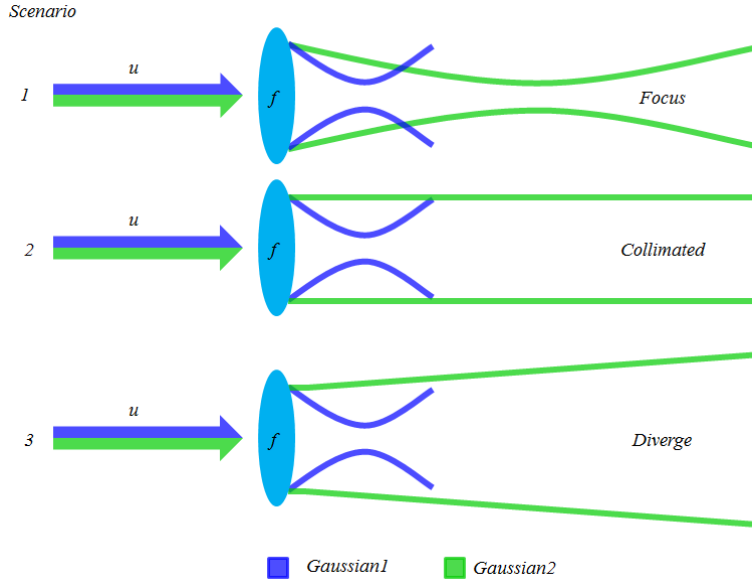


Figure 1: The three possible scenarios for the behaviour of the two Gaussian beams in the superimposed field u .

The behaviour of the CGB may be analytically determined as we are considering the superposition of two Gaussian beams of some curvature. We make use of the complex radius of curvature approach through ABCD matrices to understand the propagation of the CGB upon passing through a focusing lens. The electric field of some Gaussian beam passing through an ABCD system is given as¹⁴:

$$E(r, R) = \sqrt{\frac{2}{\pi w^2}} \frac{1}{A - B/q_1(R)} \exp\left[\frac{-i\pi r^2}{\lambda q_2(R)}\right], \quad (5)$$

with

$$\frac{1}{q_1(R)} = \frac{1}{R} - i \frac{\lambda}{\pi w^2} \quad \& \quad q_2(R) = \frac{Aq_1(R) + B}{Cq_1(R) + D}. \quad (6)$$

The equivalent ABCD matrix of the system for CGB passing through a lens of focal length f and propagating along the propagation axis, z , is given as:

$$\begin{bmatrix} A & B \\ C & D \end{bmatrix} = \begin{bmatrix} 1 & z \\ 0 & 1 \end{bmatrix} \begin{bmatrix} 1 & 0 \\ -1/f & 1 \end{bmatrix} \begin{bmatrix} 1 - z/f & z \\ -1/f & 1 \end{bmatrix}. \quad (7)$$

To obtain the final analytical expression for the field u , we substitute the matrix elements in Eq. (7) into Eq. (5 - 6) and add the two Gaussian expressions of the same width but opposite curvature which is given as:

$$u(r, R) = \frac{1}{2} (E(r, R) + E(r, -R))$$

$$= \frac{1}{2} \left(\sqrt{\frac{2}{\pi w^2}} * \frac{1}{(1-z/f) - z/q_1(R)} \exp \left[\frac{-i\pi r^2}{\lambda q_1(R)} \right] + \sqrt{\frac{2}{\pi w^2}} * \frac{1}{(1-z/f) - z/q_1(-R)} \exp \left[\frac{-i\pi r^2}{\lambda q_1(-R)} \right] \right). \quad (8)$$

The expression for the radius of curvature as in Eq. (3) is used with Eq. (8) to identify the spatial properties of the CGB. The interesting feature of the CGB as in Eq. (1) is that at the plane of the focusing lens, the number of rings is adjustable by varying the parameter N ; the OBB is always present at the focal plane of the lens independent of the input parameters and provided that a suitable value for N is selected, the CGB can operate in the regime of scenario 1 (see Fig. 1).

3. EXPERIMENTAL SETUP

The modulation of some Gaussian beam with the transmission function in Eq. (1) is performed with a phase-only SLM through complex amplitude and phase modulation^{15,16}. We considered a laser source emitting a Gaussian beam at a wavelength of 633 nm (HeNe laser) where we expanded and collimated the output beam through an eye piece lens of focal length, $f = 40$ mm, a 10X Olympus microscope objective and a lens of focal length, $f = 500$ mm. The expanded beam has a flat wavefront with an approximate diameter of ~40 mm which completely filled the active area (15.3 x 8.64 mm) of the SLM screen (Holoeye-Pluto with 1920x1080 pixels of pitch 8μm and calibrated for a 2π phase shift at 633 nm). The expanded Gaussian beam on the SLM can be approximated as a plane wave over the physical area of the transmission function as the wavefront and intensity profile over that area are flat. The SLM screen is addressed with a grey scale image of the full field as in Eq. (1) such that all the beam parameters are controlled in an all-digital approach.

The plane of the SLM is relay imaged through an afocal telescope onto a focusing lens with lenses $f = 500$ mm and $f = 500$ mm with an aperture positioned at the Fourier plane of the first lens to spatially filter the reflected beam in the selection of the first order of diffraction as is illustrated in Fig. 2. The beam thereafter is sampled along the propagation axis with a CCD camera (Spiricon Beamgage). The plane of the OBB is then relay imaged with an afocal telescope comprising of lenses $f = 200$ mm and $f = 300$ mm such that the beam can be adequately obstructed in the investigation of the bi-axial focusing property. These lenses are mounted on pop-up mounts, such that the original second focus can be sampled with or without any obstruction in the path.

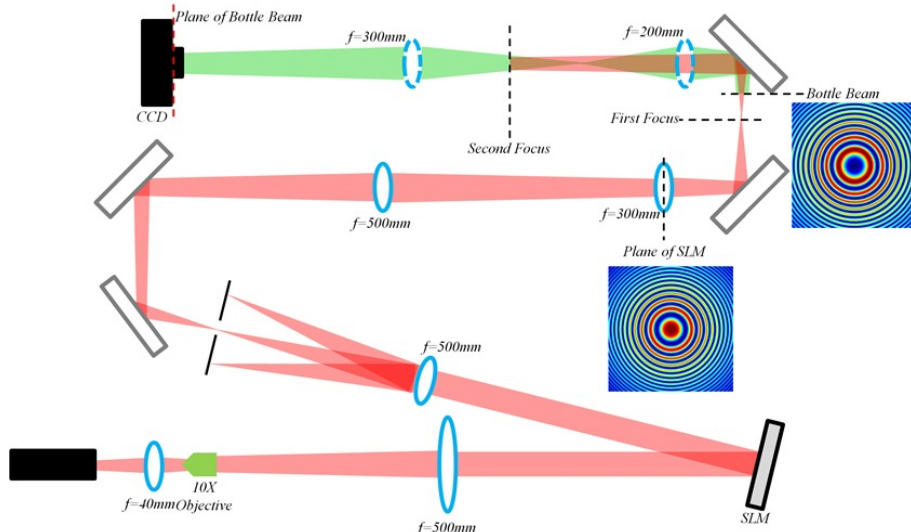


Figure 2: Experimental setup where we modulate a Gaussian beam with a transmission function of the form, $\cos(\beta r^2)$ using a SLM to generate a cosine-Gaussian beam and an optical bottle beam.

4. RESULTS AND DISCUSSION

In generating the CGB, we arbitrarily select a Gaussian width of 2.5 mm and a focusing lens of $f = 300$ mm. The condition to be satisfied using the specified Gaussian width and focusing lens such that the CGB operates in scenario 1 is $N < 16.46$ and we therefore arbitrarily select an N parameter of 11 for the discussion to follow. Owing to the interest in the bi-axial focusing property of the CGB, we theoretically determine, using Eq. (8), the on-axis intensity variation as a function of the propagation distance. As is illustrated in Fig. 3(a), there are two distinct peaks which are attributed to the two points of focus. Although there is an on-axis signal everywhere apart from the plane of the OBB, the signals when compared to the two points of focus are practically insignificant. Fig. 3(b) illustrates 2-D images of the beam at the planes of interest; the plane of the lens (CGB), the first focus, the focal plane of the lens (OBB) and the second focus.

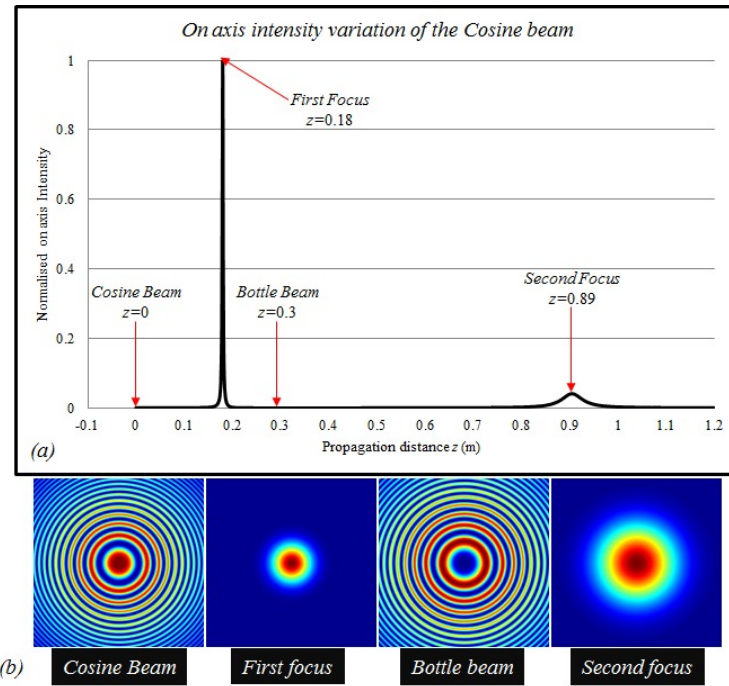


Figure 3: Theoretical determination of the (a) on-axis intensity variation of the CGB upon passing through a focusing lens and (b) 2-D intensity profiles of the beam at the planes of interest.

The parameters as mentioned above are used with Eq. (1) to address the SLM with an appropriate phase screen to obtain the CGB. Fig. 4 illustrates the beam profiles captured on the CCD device at the planes of interest and it is evident that they compare exceedingly well with the theoretical images presented in Fig. 3(b). It must be noted that from the symmetry of the starting Gaussian beams, both beams have identical divergences. At the focal plane of the lens we can infer the beam divergence through the beam sizes at this plane and since both beams have the same divergence then they both will have the same size. Although one beam is converging and the other diverging through this point, owing to their identical sizes in this plane, they will interfere with high visibility. One of the Gaussian beams will also acquire the entire Guoy phase shift thus indicating that the two Gaussian beams will have a π phase shift with respect to each other, inherently converting the cosine transmission function into a sine function. This is only valid at the focal plane of the lens which gives rise to the OBB.

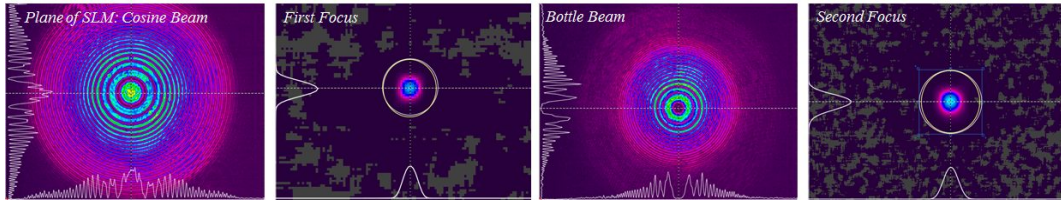


Figure 4: Experimentally obtained 2-D intensity profiles of the CGB at the planes of interest.

We explore obstructing the CGB at the plane of the OBB such that the obstruction is positioned at the intensity null. As the first focus is unaffected by the obstruction, we aim to study the effect of the obstruction on the on-axis intensity of the second focus. This effect is compared to an equivalent Gaussian beam where the curvature of the beam is selected such that it focuses in the plane of the second focus. For the unobstructed CGB (see Fig. 4), the central null of the OBB is measured to be $\sim 200 \mu\text{m}$ in diameter. Experimentally, we obstruct the beam with two circular opaque disks (of $200 \mu\text{m}$ (Fig. 5(a)) and $400 \mu\text{m}$ (Fig. 5(b))) in diameter that are fabricated by photolithography on a glass plate and analyse the on-axis intensity of their respective second foci as illustrated in Fig. 5(c-d). All the measured data of the on-axis intensity are normalised to that of the unobstructed beam which are illustrated in Fig. 5(e) for the CGB and the equivalent Gaussian beam. The variation in the on-axis intensity between the CGB and Gaussian for an obstruction diameter of $200 \mu\text{m}$ shows a significantly larger difference as compared to the $400 \mu\text{m}$ obstruction. The CGB variation from the initially unobstructed beam is very minimal (0.4%), however, for the Gaussian beam is it substantial (4.9%). By carefully selecting all parameters, including that of the obstruction diameters (variable sizes), it can be shown that the on-axis intensity of the equivalent Gaussian will decrease more rapidly with a minimal decrease in the CGB.

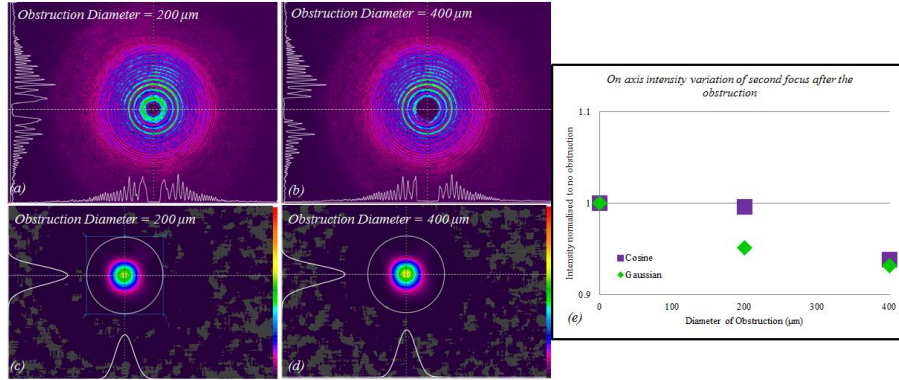


Figure 5: The CGB obstructed at the plane of the OBB with obstruction diameters of (a) $200 \mu\text{m}$ and (b) $600 \mu\text{m}$ with (c-d) their respective beams at the second point of focus. (e) The on-axis intensity variation is minimal, yet distinct when compared to an equivalent Gaussian beam.

5. CONCLUSION

We have successfully demonstrated the generation of the coaxial superposition of two Gaussian beams of equal width but opposite curvature by modulating a Gaussian beam with a transmission function of the form $\cos(\beta r^2)$, which is termed a cosine-Gaussian beam (CGB). This technique is traditionally implemented in a Mach-Zehnder interferometer; however, to avoid phase shift drift due to vibrations and thermal effects we employ amplitude and phase modulation with a spatial light modulator (SLM) to achieve the beam shaping. Upon passing the CGB through a focusing lens we have shown the generation of an optical bottle beam at the focal plane of the lens and identified bi-axial focusing. We obstructed the CGB and an equivalent Gaussian beam at the focal plane of the lens with an obstruction proportional to the size of the central null and find a variation from the initially unobstructed beam of 0.4% for the CGB and 4.9% for the equivalent Gaussian beam.

ACKNOWLEDGEMENTS

We wish to thank Dr Angela Dudley and Dr Igor Litvin for the invaluable discussions and useful advice.

REFERENCES

- [1] Dickey F. M., and Holswade S. C., [Laser beam shaping, Theory and techniques], Marcel Dekker Inc., New York, Chap. 5 and 6 (2000).
- [2] Soifer V. A., [Methods for Computer Design of Diffractive Optical Elements], John Wiley and Sons Inc., New York, Chap. 1 and 4 (2002).
- [3] Steward J. B., Saleh B. E. A., Teich M. C. and Fourkas J. T, "Experimental demonstration of polarization-assisted transverse and axial optical superresolution," Opt. Commun. 241, 315–319 (2004).
- [4] Maleev I. D., and Swartzlander G. A., "Composite optical vortices," J. Opt. Soc. Am. B. 20, 1169–1176 (2003).
- [5] Pyragaite V., and Stabinis A., "Interference of intersecting singular beams," Opt. Commun. 220, 247–255 (2003).
- [6] Ando T., Matsumoto N., Ohtake Y., Takiguchi Y., and Inoue T., "Structure of optical singularities in coaxial superpositions of Laguerre–Gaussian modes," J. Opt. Soc. Am. A. 27, 2602–2612 (2010).
- [7] Xu P., He X., Wang J. and Zhan M., "Trapping a single atom in a blue detuned optical bottle beam trap," Opt. Lett. 35, 2164–2166 (2010).
- [8] Arlt J., and Padgett M. J., "Generation of a beam with a dark focus surrounded by regions of higher intensity: the optical bottle beam," Opt. Lett. 25, 191–193 (2000).
- [9] Tai P. T., Hsieh W. F. and Chen C. H., "Direct generation of optical bottle beams from a tightly focused end-pumped solid-state laser," Opt. Exp. 12, 5827–5833 (2004).
- [10] Chen C. H., Tai P. T. and Hsieh W. F., "Bottle beam from a bare laser for single-beam trapping," Appl. Opt. 43, 6001–6006 (2004).
- [11] Ahluwalia B. P. S., Yuan X. C. and Tao S. H., "Generation of self-imaged optical bottle beams," Opt. Commun. 238, 177–184 (2004).
- [12] Isenhower L., Williams W., Dally A. and Saffman M., "Atom trapping in an interferometrically generated bottle beam trap," Opt. Lett. 34, 1159–1161 (2009).
- [13] Boubaha B., Naidoo D., Godin T., Fromager M., Forbes A. and Aït-Ameur K., "Spatial properties of coaxial superposition of two coherent Gaussian beams," Appl. Opt. 52(23), 5766 – 5772 (2013).
- [14] Hodgson N., and Weber H., [Laser Resonators and Beam Propagation], Springer, New York, Chap. 2 (2005).
- [15] Arrizón V., Ruiz U., Carrada R., and González L. A., "Pixelated phase computer holograms for the accurate encoding of scalar complex fields." J. Opt. Soc. Am. A 24, 3500–3507 (2007).
- [16] Flamm D., Naidoo D., Schulze C., Forbes A., and Duparré M., "Mode analysis with a spatial light modulator as a correlation filter," Opt. Lett. 37, 2478–2480 (2012).